Medicine®

OPEN

Assessment of therapeutic response in Crohn's disease using quantitative dynamic contrast enhanced MRI (DCE-MRI) parameters
A preliminary study

Jianguo Zhu, MD, PhD[a], Faming Zhang, MD[b], Jinfa Zhou, MD[a], Haige Li, MD[a],*

Abstract

The aim of the study was to investigate dynamic contrast enhanced MRI (DCE-MRI) as a potential marker to assess the therapeutic responses of fecal microbiota transplantation (FMT) in patients with Crohn's disease (CD) and to determine the parameter or combination of parameters most strongly associated with changes in clinical indicators after treatment.

In 22 CD patients, DCE-MRI was performed with a 3.0T scanner. Parameters of DCE-MRI (vascular transfer constant [K^{trnas}] and blood volume [BV]) in the terminal ileum were compared between before and day 90 after FMT treatment. The differences of clinical indicators (C-reactive protein [CRP], Harvey–Bradshaw index [HBI]) and DCE-MRI parameters (K^{trnas}, BV) between pre- and post-treatment was calculated by Student's 2-tailed, paired t-test. The correlations between percent change of clinical indicators (ΔCRP, ΔHBI) with DCE-MRI parameters (ΔK^{trnas}, ΔBV) were analyzed by Pearson's correlation coefficients. A logistic regression model was used to identify the changes of DCE-MRI parameters related to the treatment outcomes. Receiver operating characteristic curves (ROCs) were generated to assess which DCE-MRI parameter showed the best accuracy for evaluation of therapeutic response.

After treatment, mean values of clinical indicators decreased significantly (CRP: 62.68 ± 31.86 vs 43.55 ± 29.63 mg/L, $P = .008$; HBI: 7.18 ± 2.10 vs 5.73 ± 2.33, $P = 0.012$). Both DCE-MRI parameters showed prominent differences before and after treatment: K^{trans} (1.86 ± 0.87 vs 1.39 ± 0.83 min^{-1}, $P = .017$), BV (61.02 ± 28.49 vs 41.96 ± 22.75 mL/100 g, $P = .005$). There were significant correlations between ΔCRP or ΔHBI and percent change of CDE-MRI parameters (ΔK^{trans} to ΔCRP: 0.659; ΔK^{trans} to ΔHBI: 0.496; ΔBV to ΔCRP: 0.442; ΔBV to ΔHBI: 0.476). Compared to ΔK^{trans} and ΔBV individually, the combination of both parameters performed best in assessment of therapeutic response with an area under the ROCs (AUC) of 0.948.

K^{trans} and BV parameters derived from DCE-MRI have the potential to assess for therapeutic response after FMT treatment for CD. The combination of K^{trans} and BV measurements improved the predictive capability compared to the individual parameters.

Abbreviations: BV = blood volume, CD = Crohn's disease, CRP = C-reactive protein, DCE-MRI = dynamic contrast-enhanced MRI, FMT = fecal microbiota transplantation, HBI = Harvey–Bradshaw index, ICC = intraclass correlation coefficient, K^{trans} = volume transfer coefficient reflecting vascular permeability, MRI = magnetic resonance imaging, ROC = receiver operating characteristic, ROI = region of interest, SDs = standard deviations.

Keywords: blood volume, Crohn's disease, dynamic contrast enhanced MRI, therapeutic responses, vascular transfer constant

1. Introduction

Crohn's disease (CD) is a type of inflammatory bowel disease (IBD) with uncertain etiology. CD can affect any area of the gastrointestinal tract from the mouth to the rectum and anus. The terminal ileum is the most vulnerable region in CD and ileocecal CD often leads to serious complications such as strictures and perforation.[1] The incidence and prevalence of CD vary between geographical areas. In mainland China, data published in 2011 have shown an incidence of 1.21 cases per 100,000 persons with the prevalence estimated about 2.29 cases/100,000 people.[2]

CD is characterized by high rates of recurrence. Currently, there are limited treatment options for CD. Patients with CD have a chronic disease that requires ongoing follow-up.

Endoscopy remains the reference standard. However, conventional endoscopy is invasive, shows limited evaluation of the small bowel, and requires sedation/anesthesia during the procedure.[3] Clinical scores such as Crohn's disease activity index (CDAI) and Harvey–Bradshaw index (HBI) are easy and commonly used for CD evaluation.[4] But the scores are based on subjective criteria. Due to the nature of its rapid response and short half-life, C-reactive protein (CRP) acts as a useful marker of inflammation especially in the management of CD.[5] But the CRP level is dependent on the site and number of active CD lesions, and is therefore not specific.[6,7]

Recently, magnetic resonance imaging (MRI) has become the primary imaging tool for evaluation of disease activity in patients with CD because of the advantages of lack of ionizing radiation exposure and the ability to assess for both intestinal and extra-intestinal disease activity.[8–10] Compared with conventional

imaging, newly emerging functional techniques such as dynamic contrast enhanced MRI (DCE-MRI) provide advantages in extraction of lesion mechanisms and offer more physiological information.

DCE-MRI is currently used to evaluate treatment responses for malignant tumors including glioblastoma,[11] multiple myeloma,[12] breast cancer,[13] pancreatic cancer,[14] and prostatic carcinoma.[15] Meanwhile, studies have employed this technique to assess neovascularization in inflammatory diseases.[16,17] We have assessed the role of DCE-MRI in diagnosis and assessment for CD,[18] such findings are similar to other researches.[19–21] In this paper, we present a preliminary study of CD by DCE-MRI and hypothesize that the parameters of DCE-MRI can be used to evaluate the therapeutic response.

2. Material and methods

This research was conducted from June 1, 2014, to January 31, 2016. All patients agreed to participate in a clinical trial of FMT for CD (NCT01793831) at The Second Affiliated Hospital of Nanjing Medical University. Twenty-two patients with CD (13 men and 9 women; age range 19–62 years, mean $\pm$ SD $=33.45 \pm 11.39$ years) were enrolled into the study. Inclusion criteria for this study were as follows: (1) first-visit subjects with complaints of digestive disorder; (2) adults aged 18 years or older; (3) underwent capsule enteroscopy and colonoscopy within the past 72 hours; (4) CD diagnosis confirmed by endoscopy and pathology; (5) only one lesion, and located at the terminal ileum; (6) ability to undergo MRI. This study was approved by the institutional review board. Informed consent was obtained from all patients.

2.1. Trial design

All patients with CD underwent MRI scanning twice. The first scan was prior to single fecal microbiota transplantation (FMT) treatment and the second scan was performed on day 90 after the initiation of the treatment. At the 2 time points, clinical data including laboratory examination, clinical scores and endoscopy were also collected. The changes in CRP and HBI were used as clinical indicators of disease progression. Serum samples were obtained from each subject for analysis of CRP prior to MRI scanning within the same day. The severity score for CD was defined and endoscopy was performed within 72 hours before MRI examination. DCE-MRI parameters were measured in the ileocecal region. Therapeutic response of each patient was assessed by correlating imaging parameters with clinical data.

2.2. MRI study protocol

MRI scan was performed using a 3.0 T clinical scanner (SignaHDxt, GE Healthcare) equipped with abdominal-pelvic coil (8 radio frequency channels). Subjects were scanned in supine position. No special preparation was required other than withholding intake of solid foods for 6 hours prior to MRI examination. All subjects were required to drink 300 mL of mannitol (2.5%) every 10 minutes until a total of 1.5 L has been consumed within 60 minutes. Immediately prior to the scan, all individuals were given of 20 mg of scopolamine-N-butyl bromide (Busco-pan; BoehringerIngelheim, Ingelheim, Germany) intravenously, to reduce bowel peristalsis motion artifacts.

Morphologic sequences and scan parameters were: (1) coronal T2 (single shot fast spin-echo, SSFSE) through the abdomen and pelvis with breath-holding (Tck $=5$ mm, spacing $=1$ mm; TR $=$ 2800 ms, TE $=70$ ms); (2) axial T2 fast spin-echo fat-suppressed images covering the abdomen and pelvis, free-breathing with navigator triggering (Tck $=4$ mm, spacing $=2$ mm; TR $=12000$ ms, TE $=90$ ms); (3) axial T1 LAVA-Flex Mask through the abdomen and pelvis with breath-holding (Tck $=4$ mm, spacing $=$ 0 mm; TR $=4.5$ ms, TE $=1.7$ ms).

DCE-MRI protocol included 2 steps: (1) 5 different flip angles (4°, 6°, 8°, 10°, and 12°) T1-weighted 3D-LAVAsequences to determine the T1 relaxation time in the blood and tissue for T1 mapping; (2) DCE-MRI using 3D T1-weighted LAVA sequence with a flip angle of 12°. After 3 pre-contrast acquisitions, Gadodiamide (OmniScan, GE Healthcare, Ireland) was intravenously injected (0.2 mmol/kg) with a rate of 3.0 mL/s. Then, 15 mL of saline was flushed with the same rate. Scan parameters were following: axial images; TR $=2.9$ ms, TE $=1.1$ ms; matrix $=$ 224×160; FOV $=42$ cm; scan layers $=52$. The temporal resolution was 7 seconds and the total scan time was 3 minutes 30 seconds including 30 phases. According to the inclusion criteria for this study, the terminal ileum was chosen as DCE-MRI scanning reference slice.

2.3. Interpretation of MRI measurements

DCE-MRI parameters were calculated using a noncommercial software (Omni-Kinetics, GE Healthcare). First, the individual artery input function (AIF) was obtained from a region of interest (ROI) drawn on the abdominal aorta located in close proximity to the terminal ileum. Second, extended Tofts liner model was chosen for fitting of the tissue response curves.[22] The pharmacokinetic parameter as K^{trans} and hemodynamic parameter as BV were generated as color maps (Fig. 1). ROI (30–50 mm^2) for these DCE-MRI parameters (K^{trans}, BV) was placed on the maximal enhancing region of the terminal ileum.

2.4. Quantitative measurement

Response to treatment was determined by the change in CRP and HBI. For each subject, percent changes in CRP and HBI between baseline and 90-day follow-up was calculated using the following equation:

ΔCRP (%) $=[($CRP$_{90days} -$ CRP$_{baseline})/$ CRP$_{baseline}] \times 100$

ΔHBI (%) $=[($HBI$_{90days} -$ HBI$_{baseline}) /$ HBI$_{baseline}] \times 100$

Percent changes in DCE-MRI parameters relative to baseline were calculated as follows:

ΔK^{trans}(%) $=[(K^{trans}{}_{90days} - K^{trans}{}_{baseline}) / K^{trans}{}_{baseline}] \times 100$

ΔBV (%) $=[($BV$_{90days} -$ BV$_{baseline}) /$ BV$_{baseline}] \times 100$

2.5. Reproducibility of DCE-MRI parameter measurements

All parameters in DCE-MRI were independently evaluated by 2 radiologists (with a combined 10 years of body MRI experience), who were blinded to the clinical and endoscopic examination. To further assess the reproducibility and the repeatability of the measurements, Bland–Altman plots were generated and intra-class correlation coefficient (ICC) was calculated. In the graphic method, the differences between the 2 radiologists are plotted against the averages of the 2 radiologists. Agreement was classified as excellent (ICC > 0.75), moderate (ICC $=0.50–0.75$), or poor (ICC < 0.50). The mean of the 2 values (measured by different radiologists) was accepted as the final result for the quantitative analysis.
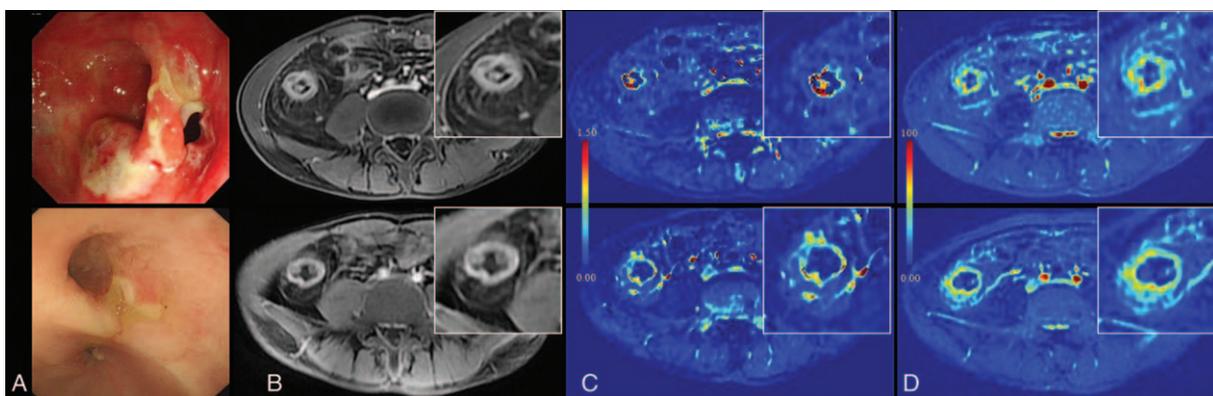
Figure 1. Comparison of endoscopic and MRI images. Endoscopic (A); enchanced TI-weighted (B); K^{trans} (C); BV (D) images of patient 1 acquired pretreatment and post-treatment. Top, pretreatment; bottom, post-treatment. BV=blood volume, K^{trans}=vascular transfer constant, MRI = magnetic resonance imaging.

2.6. Statistical analysis

First, all data in both clinical (CRP, HBI) and DCE-MRI (K^{trans}, BV) were tested with the Kolmogorov–Smirnov test for normal distribution before analysis. Normally distributed data were expressed as mean and standard deviations (SDs), whereas non-normally distributed data were expressed as median and interquartile ranges (IQRs). Second, intrameasurement reproducibility of the DCE-MRI was assessed through the calculation of ICC. Third, for normally distributed data, Student's 2-tailed, paired t-test was used to test statistical significance of change from pre- to post-treatment for each parameter (Levene's test for homogeneity was conducted first to test the assumption of equal variance). Pearson's correlation coefficients were used to measure the strength of the relationship between each percent change of DCE-MRI parameters and CRP, HBI in CD patients. For data not normally distributed, nonparametric tests were used such as the Mann–Whitney test for pre- and post-treatment comparisons and Spearman analysis for correlation. Lastly, a logistic regression model was used to identify the changes of DCE-MRI parameters related to the treatment outcomes. Receiver operating characteristic curves (ROCs) were generated to assess which DCE-MRI parameter showed the best accuracy for evaluation of therapeutic response. Optimal cut-off values of each DCE-MRI parameter and combination of parameters for identification of good or poor treatment outcome (based on the changes of CRP and HBI between pre- and post-treatment) were determined. Areas under the ROCs (AUC) were derived to estimate the probability of correctly assessment of therapeutic response.

All the computations were performed using SPSS (version 18.0; IBM SPSS Inc., Chicago, IL). Statistical significance was set at $P < .05$.

3. Results

Twenty-two patients who received FMT for CD were analyzed in this study (Table 1). All parameters in both clinical and DCE-MRI were normally distributed, means and SDs were provided for continuous variable in this study (Table 2).

3.1. Comparison of changes in the clinical data after treatment

The mean value of CRP decreased significantly ($P = .008$) from 62.68 ± 31.86 mg/L (range 19–121 mg/L) to 43.55 ± 29.63 mg/L (range 5–135 mg/L) on day 90 after FMT treatment. Percent change in the CRP value was -22.44 ± 43.65%. In parallel, HBI

showed an analogous decline ($P = .012$) from baseline (mean 7.18 ± 2.10, range 3–11) to day 90 (mean 5.73 ± 2.33, range 3–11), and the change in HBI was −15.86 ± 36.48%. Among all 22 subjects, 6 patients were considered to have poor treatment outcomes due to increased CRP and HBI values compared to pretreatment (Fig. 2).

3.2. Reproducibility of MRI parameter measurements

There were 88 MRI sets in total including 44 sets for K^{trans} (each 22 sets in pre- and post-treatment) and 44 sets for BV (each 22 sets in pre- and post-treatment). K^{trans} and BV showed ICC values of 0.990 (95% confidence interval [CI], 0.981– 0.994) and 0.999 (95% CI, 0.998 – 0.999), respectively. The Bland–Altman plots suggested that interobserver agreement was high (Fig. 3).

Table 1

The characteristics of included patients.

Items	Results
Total number	22
Age, mean ± SD, range	33.45 ± 11.39 (19–62)
Sex, male %, n	59.1 (13)
Location, %, n	
Terminal ileum	100 (22)
Using immunomodulator, yes %, n	0 (0)
Using steroid, yes %, n	0 (0)
Using anti-TNF, yes %, n	0 (0)
With history of surgery, yes %, n	0 (0)

SD = standard deviation.

Table 2

Comparisons of clinical indicators and DCE-MRI parameters before and after treatment.

	Pre-treatment	Post-treatment	P
CRP, mg/L	62.68 ± 31.86	43.55 ± 29.63	.008
HBI	7.18 ± 2.10	5.73 ± 2.33	.012
K^{trans}, min^{-1}	1.86 ± 0.87	1.39 ± 0.83	.017
BV, mL/100 g	61.02 ± 28.49	41.96 ± 22.75	.005

n = 22.
All continuous data are normally-distributed. Means and SDs are provided for continuous variable.
P value is obtained by Student's 2-tailed, paired t-test.
BV = blood volume, CRP = C-reactive protein, DCE-MRI = dynamic contrast-enhanced MRI, HBI = Harvey–Bradshaw index, K^{trans} = vascular transfer constant.
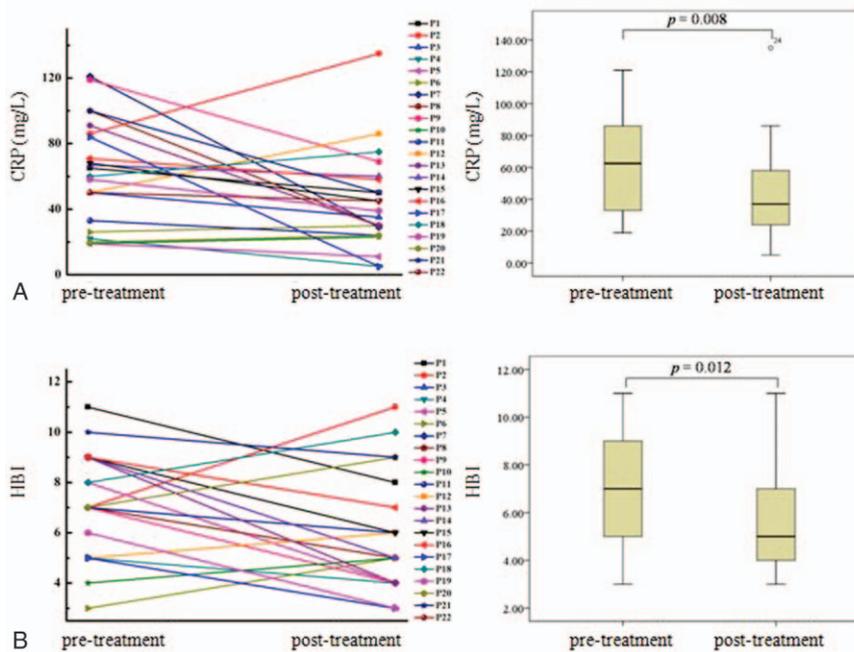
Figure 2. Changes of CRP and HBI after treatment. Among all 22 subjects, 6 patients (patient 2, 6, 10, 12, 18, and 20) are considered to have poor treatment outcomes due to increased CRP and HBI values compared to pretreatment. CRP = C-reactive protein, HBI = Harvey–Bradshaw index, P = patient.

3.3. Comparison of changes in the DCE-MRI parameters after treatment

The following parameters were significantly different before and after treatment: K^{trans} (1.86 ± 0.87 vs 1.39 ± 0.83 min^{-1}; $P = .017$), BV (61.02 ± 28.49 vs 41.96 ± 22.75 mL/100 g; $P = .005$). Relative percent changes in K^{trans} and BV on day 90 after treatment were –24.94 ± 46.07% and –21.29 ± 45.69%. After treatment, increased values of K^{trans} and BV were showed in 6 and 5 patients respectively (Fig. 4).

3.4. Correlation of DCE-MRI parameters with clinical indicators after treatment

ΔK^{trans} and ΔBV were correlated with ΔCRP (Pearson correlation coefficient: $r = 0.659$, $P = .001$; $r = 0.442$, $P = .039$). There were also positive correlations between the change of MRI parameters

and HBI, such as ΔK^{trans} to ΔHBI ($r = 0.496$, $P = .019$), and ΔBV to ΔHBI ($r = 0.476$, $P = .025$). ΔK^{trans} showed higher correlation with the percent changes of clinical indicators than ΔBV (Fig. 5).

3.5. Comparison of assessment efficacy among the DCE-MRI parameters

According to the changes of clinical indicators after treatment, 22 subjects were divided to good (16 subjects with decreased clinical indicators) and poor treatment outcomes (6 subjects with increased clinical indicators). Bivariate logistic regression model was used to estimate the interaction of DCE-MRI parameters and treatment outcomes. ΔK^{trans} [odds ratio (OR) 0.010, 95% CI 0.000–0.521, $P = .023$] and ΔBV (OR 0.023, 95% CI 0.001–0.920, $P = .045$) were associated with treatment outcomes. The sensitivity of predicting the therapeutic response was
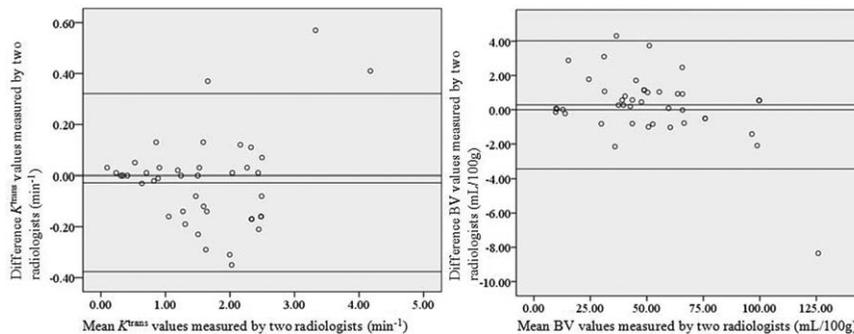
Figure 3. Bland–Altman plots of 2 radiologists' measurements. Bland–Altman 95% limits of agreement in MRI parameters including K^{trans} and BV. Top dotted line shows the upper limit of agreement (mean difference plus 1.96 times standard deviation); bottom line shows a lower limit of agreement (mean difference minus 1.96 times standard deviation). Plots show a possible relationship between 2 radiologists in measurements. BV = blood volume, K^{trans} = vascular transfer constant, MRI = magnetic resonance imaging.
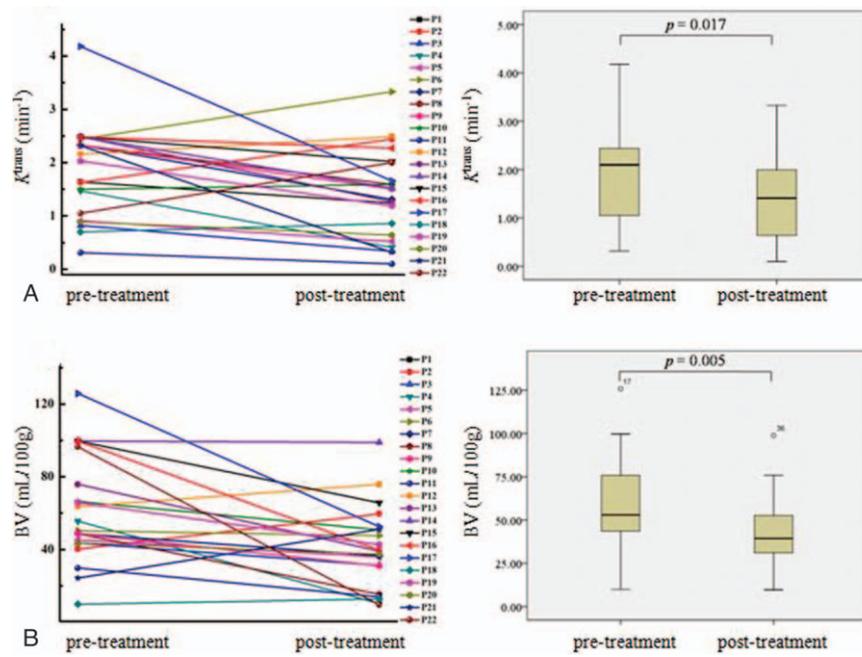
Figure 4. Changes of K^{trans} and BV after treatment. Increased values of K^{trans} and BV are showed in 6 (patient 2, 6, 10, 12, 18, and 22) and 5 (patient 1, 2, 12, 18, and 21) patients, respectively. BV = blood volume, K^{trans} = vascular transfer constant, P = patient.

83.3% when ΔK^{trans} was −2%, and the specificity was 93.7%, both of which were calculated with the values for ΔBV (cut-off = −24.46%; sensitivity of 100% and specificity of 75.0%). The AUC of 0.906 for ΔK^{trans} was slightly higher than the AUC for ΔBV (0.865). However, when ΔK^{trans} and ΔBV were combined, a considerably higher sensitivity (81.3%) and specificity (100%) with a significant discriminative accuracy (AUC = 0.948) was found (Fig. 6).
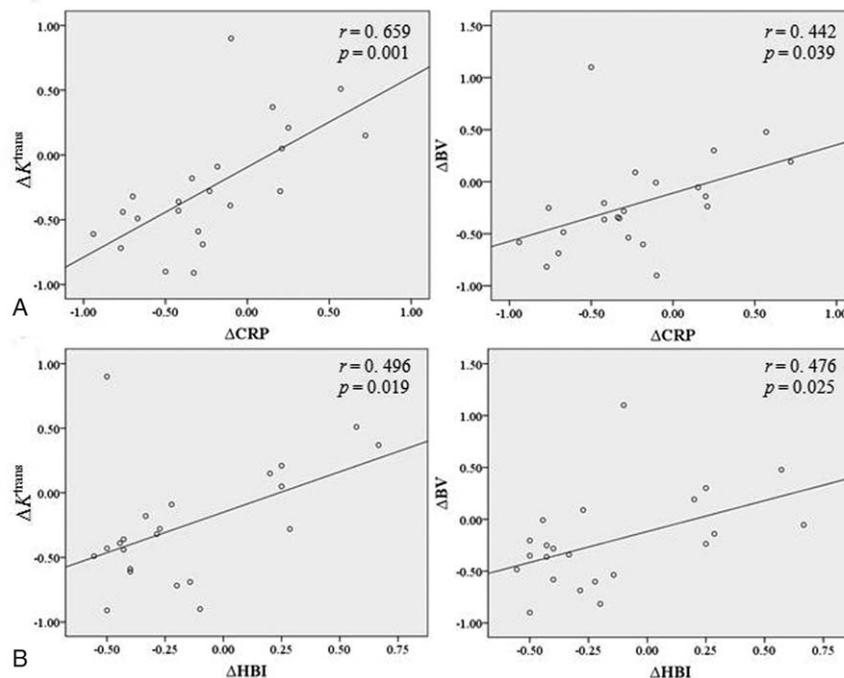
Figure 5. The relationship between DCE-MRI parameters and clinical indicators after treatment. ΔK^{trans} and ΔBV are correlated with ΔCRP (Pearson correlation coefficient: $r = 0.659$, $P = .001$; $r = 0.442$, $P = .039$) (A). Scatter plots depict the positive correlations between ΔK^{trans} or ΔBV and ΔHBI ($r = 0.496$, $P = .019$; $r = 0.476$, $P = .025$) (B). ΔK^{trans} shows higher correlation with the percent changes of clinical indicators than ΔBV. BV = blood volume, CRP = C-reactive protein, HBI = Harvey–Bradshaw index, K^{trans} = vascular transfer constant, ΔCRP (%) = [(CRP $_{90\ days}$ −CRP $_{baseline}$)/CRP $_{baseline}$] × 100, ΔHBI (%) = [(HBI $_{90days}$ −HBI $_{baseline}$)/HBI $_{baseline}$] × 100, ΔK^{trans} (%) = [(K^{trans}_{90days} −$K^{trans}_{baseline}$)/$K^{trans}_{baseline}$] × 100, ΔBV (%) = [(BV$_{90days}$ −BV$_{baseline}$)/BV$_{baseline}$] × 100.
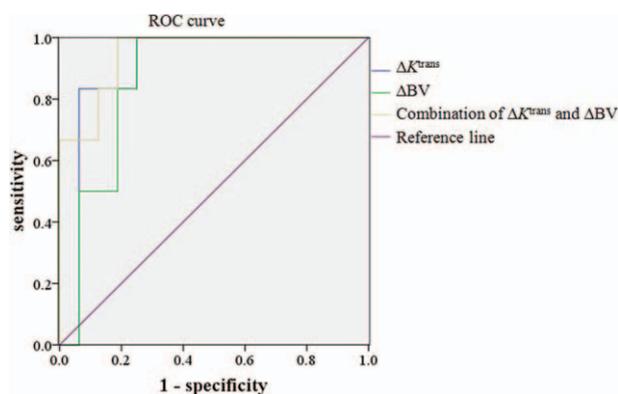
Figure 6. The assessment efficacy of different MRI parameters for therapeutic response to treatment. The area under the curve is 0.906 for ΔK^{trans}, 0.865 for ΔBV. ROC analysis reveals the combination of ΔK^{trans} and ΔBV to perform best in assessment of therapeutic response (0.948). BV = blood volume, K^{trans} = vascular transfer constant, ROC = receiver operating characteristic, ΔCRP (%) = [(CRP $_{90days}$ −CRP $_{baseline}$)/CRP $_{baseline}$] × 100, ΔHBI (%) = [(HBI $_{90days}$ −HBI $_{baseline}$)/HBI $_{baseline}$] × 100.

4. Discussion

4.1. Current research status about DCE-MRI in the assessment of therapeutic response

By a serial acquisition of T1weighted images before, during, and after the injection of a paramagnetic contrast agent, meaningful physiological parameters related to vessel volume and permeability can be calculated. Thus, DCE-MRI has the potential to serve as an imaging biomarker of the clinical therapeutic response especially in tumors to antivascular therapies. De Bruyne S et al[23] assessed the role of DCE-MRI for evaluation of response to chemotherapy and bevacizumab and for prediction of progression-free survival in 19 patients with colorectal liver metastases. They concluded a decrease in K^{trans} (>40%) was a favorable prognostic factor. Pishko et al[24] applied K^{trans} and BV as biomakers to investigate the effect of treatment in a rat model of human lung cancer brain metastasis. Recently, DCE-MRI has been applied for the detection of inflammatory diseases and assessment of the therapeutic response to treatment of inflammatory diseases. Liu et al[16] evaluated DCE-MRI for assessment of perfusion in 10 rheumatoid arthritis patients. They found that DCE-MRI parameters correlated significantly with treatment responses between baseline and follow-up. Floc'h et al[25] reported the use of DCE-MRI to quantify changes in vascular permeability in a guinea-pig model of inner ear inflammation. These studies have demonstrated that DCE-MRI has the potential to become an accepted noninvasive indicator of vascularity and therefore ultimately, a biomarker of treatment response.

4.2. Why to choose CRPand HBI as reference index in this study

In most experimental and clinical studies, histological tissue sections are set as gold-standard to validate the reliability of DCE-MRI parameters in predicting outcomes related to therapy. For example, Chen et al[26] evaluated the correlation between parameters of DCE-MRI and microvessel density (MVD) measurements in rabbit VX2 liver tumor models. Jia et al[27] used pathological complete response and major histological response as

references to identify the capability of DCE-MRI in predicting treatment response among 48 breast cancer patients. In the current study, choosing CRP and HBI as reference was based on following reasons: (1) surgery is not the preferred treatment for CD, so it is difficult to obtain pathological samples; (2) MVD reports only a morphologic index of vasculature and cannot differentiate between functional vessels, whereas DCE-MRI parameters reflect those vessels with active perfusion[28]; (3) CRP and clinical scores have been set as gold-standard in previous DCE-MRI researches[16,18]; (4) CRP and HBI are important monitoring tools in the clinical management of CD.[29,30]

4.3. The value of DCE-MRI parameters in this study

In CD pathogenesis, angiogenesis activated primarily by hypoxia is clearly related to inflammation.[31] Some researchers[32,33] even emphasize that angiogenesis could play a key role as a cause of CD tissue injury and driving force of inflammation. Several alternate processes including the cell-to-extracellular matrix interaction, vessel wall maturation, and basal lamina modifications are implicated in new vessel development. Multiple new blood vessels gather together to build vascular nets. The process of new blood vessels forming is known as angiogenesis. Based on the above analysis, it is well established that in CD, angiogenesis represents microvascular remodeling which leads to increased vascular wall permeability, this in turn increases exudation from vessels into the extravascular extracellular space (EES); vascular density changes whereby blood flow increases.[34] By changing the fecal dysbiosis, FMT as a safe, feasible, and efficient therapy that could help reduce intestinal inflammation and inhibit angiogenesis.[35,36]

The volume transfer constant of contrast agent from a plasma space to an EES, as defined K^{trans}, has been used to characterize this microvascular permeability quantitatively. Another significant parameter: BV has been applied to calculate blood density and blood flow. In this study, K^{trans} and BV decreased significantly after treatment and good correlation was shown between ΔK^{trans}, ΔBV, and changes of clinical indicators. In our prior study,[18] we have found the parameters of DCE-MRI including K^{trans} had significant correlation with CRP. Sinha et al[37] concluded that the contrast agent rapidly passed from the vascular space into the EES, resulting in mural enhancement in CD patients. According to the above conclusions, we hypothesized that K^{trans} as a pharmacokinetic parameter can reflect the change of microvascular permeability and may add valuable information about disease severity in CD. The current study also demonstrated the mean value of BV differed significantly between pre- and post-treatment. Similar results can be found in other research. For example, Nylund et al[38] made a comparison of BV between CD patients with inflammation or fibrosis using contrast-enhanced ultrasound. They reported the fibrosis group had lower BV compared with the inflammation group ($P = .001$). These findings suggested BV as a perfusion parameter can assess the bowel wall vascularization and monitor therapeutic responses to treatment.

Furthermore, we demonstrated that when comparing K^{trans} with BV, ΔK^{trans} performed better in assessment of therapeutic response than ΔBV. Similar results were also observed in a previously reported study.[39] Keeping in mind that K^{trans} reflects vascular permeability, whereas BV is influenced more by the number and density of microvessels,[28] a few possible explanations should be considered. First, anatomic vascular changes in response to treatment are found to occur at a later point than

changes in vascular permeability.[40] Second, based on the pharmacokinetic model, K^{trans} is less affected than BV by the molecular weight of the contrast agent and is therefore more accurate.[39]

As described above, DCE-MRI is a method for characterization of angiogenic activity in CD. DCE-MRI parameters (K^{trans} and BV) can provide quantitative information about the volume and permeability of these new vessels. By the combination of both parameters, a logistic regression equation was developed to generate a combination predicting factor for assessment of therapeutic responses. The AUC of the combined K^{trans} and BV was higher than its individual components, indicating that both parameters together reflect comprehensive treatment response-related information.

Several limitations were present in this study: First, the study included data from a small number of patients. Second, we cannot obtain pathological specimens by FMT treatment, so the comparative analysis between pathology and DCE-MRI parameters was lacking. Our third limitation was due to the technique: currently, we cannot employ DCE-MRI to assess CD patients with multiple lesions, so the patients included were restricted to only 1 lesion and located only at the terminal ileum.

5. Conclusion

The DCE-MRI quantitative parameters (K^{trans} and BV) could be used to precisely evaluate the therapeutic response of CD lesions after FMT therapy. As a promising inflammation quantification tool in clinical research of CD, DCE-MRI may contribute unique insights into the response of the lesion microenvironment to therapy. Therefore, we believe that DCE-MRI quantitative analysis technology might have broad applications in the field of precision medicine.

References

[1] Nystrom N, Berg T, Lundin E, et al. Human enterovirus species B in ileocecal Crohn's disease. Clin Transl Gastroenterol 2013;4:e38.

[2] Zheng JJ, Shi XH, Zhu XS, et al. A comparative study of incidence and prevalence of Crohn's disease in mainland China in different periods. Zhonghua Nei Ke Za Zhi 2011;50:597–600.

[3] Sauer CG, Middleton JP, McCracken C, et al. Magnetic resonance enterography healing and magnetic resonance enterography remission predicts improved outcome in pediatric Crohn disease. J Pediatr Gastroenterol Nutr 2016;62:378–83.

[4] Sun H, Papadopoulos EJ, Hyams JS, et al. Well-defined and reliable clinical outcome assessments for pediatric Crohn disease: a critical need for drug development. J Pediatr Gastroenterol Nutr 2015;60:729–36.

[5] Zhu W, Guo Z, Zuo L, et al. CONSORT: different end-points of preoperative nutrition and outcome of bowel resection of Crohn disease: a randomized clinical trial. Medicine (Baltimore) 2015;94:e1175.

[6] Horsthuis K, Lavini C, Bipat S, et al. Perianal Crohn disease: evaluation of dynamic contrast-enhanced MR imaging as an indicator of disease activity. Radiology 2009;251:380–7.

[7] Wiskin AE, Wootton SA, Cornelius VR, et al. No relation between disease activity measured by multiple methods and REE in childhood Crohn disease. J Pediatr Gastroenterol Nutr 2012;54:271–6.

[8] Kulkarni S, Gomara R, Reeves-Garcia J, et al. MRI-based score helps in assessing the severity and in follow-up of pediatric patients with perianal Crohn disease. J Pediatr Gastroenterol Nutr 2014;58:252–7.

[9] Shenoy-Bhangle A, Nimkin K, Goldner D, et al. MRI predictors of treatment response for perianal fistulizing Crohn disease in children and young adults. Pediatr Radiol 2014;44:23–9.

[10] Mollard BJ, Smith EA, Dillman JR. Pediatric MR enterography: technique and approach to interpretation-how we do it. Radiology 2015;274:29–43.

[11] Blasel S, Zagorcic A, Jurcoane A, et al. Perfusion MRI in the evaluation of suspected glioblastoma recurrence. J Neuroimaging 2016;26:116–23.

[12] Dutoit JC, Claus E, Offner F, et al. Combined evaluation of conventional MRI, dynamic contrast-enhanced MRI and diffusion weighted imaging for response evaluation of patients with multiple myeloma. Eur J Radiol 2016;85:373–82.

[13] Chang RF, Chen HH, Chang YC, et al. Quantification of breast tumor heterogeneity for ER status, HER2 status, and TN molecular subtype evaluation on DCE-MRI. Magn Reson Imaging 2016;34:809–19.

[14] Kim JH, Kim H, Kim YJ, et al. Dynamic contrast-enhanced ultrasonographic (DCE-US) assessment of the early response after combined gemcitabine and HIFU with low-power treatment for the mouse xenograft model of human pancreatic cancer. Eur Radiol 2014;24:2059–68.

[15] Barrett T, Gill AB, Kataoka MY, et al. DCE and DW MRI in monitoring response to androgen deprivation therapy in patients with prostate cancer: a feasibility study. Magn Reson Med 2012;67:778–85.

[16] Liu J, Pedoia V, Heilmeier U, et al. High-temporospatial-resolution dynamic contrast-enhanced (DCE) wrist MRI with variable-density pseudo-random circular Cartesian undersampling (CIRCUS) acquisition: evaluation of perfusion in rheumatoid arthritis patients. NMR Biomed 2016;29:15–23.

[17] Chen H, Wu T, Kerwin WS, et al. Atherosclerotic plaque inflammation quantification using dynamic contrast-enhanced (DCE) MRI. Quant Imaging Med Surg 2013;3:298–301.

[18] Zhu J, Zhang F, Luan Y, et al. Can dynamic contrast-enhanced MRI (DCE-MRI) and diffusion-weighted MRI (DW-MRI) evaluate inflammation disease: a preliminary study of Crohn's disease. Medicine (Baltimore) 2016;95:e3239.

[19] Tielbeek JA, Ziech ML, Li Z, et al. Evaluation of conventional, dynamic contrast enhanced and diffusion weighted MRI for quantitative Crohn's disease assessment with histopathology of surgical specimens. Eur Radiol 2014;24:619–29.

[20] Yacoub JH, Oto A. New magnetic resonance imaging modalities for Crohn disease. Magn Reson Imaging Clin N Am 2014;22:35–50.

[21] Oto A, Kayhan A, Williams JT, et al. Active Crohn's disease in the small bowel: evaluation by diffusion weighted imaging and quantitative dynamic contrast enhanced MR imaging. J Magn Reson Imaging 2011;33:615–24.

[22] Sourbron SP, Buckley DL. On the scope and interpretation of the Tofts models for DCE-MRI. Magn Reson Med 2011;66:735–45.

[23] De Bruyne S, Van Damme N, Smeets P, et al. Value of DCE-MRI and FDG-PET/CT in the prediction of response to preoperative chemotherapy with bevacizumab for colorectal liver metastases. Br J Cancer 2012;106:1926–33.

[24] Pishko GL, Muldoon LL, Pagel MA, et al. Vascular endothelial growth factor blockade alters magnetic resonance imaging biomarkers of vascular function and decreases barrier permeability in a rat model of lung cancer brain metastasis. Fluids Barriers CNS 2015;12:5.

[25] Floc'h JL, Tan W, Telang RS, et al. Markers of cochlear inflammation using MRI. J Magn Reson Imaging 2014;39:150–61.

[26] Chen J, Qian T, Zhang H, et al. Combining dynamic contrast enhanced magnetic resonance imaging and microvessel density to assess the angiogenesis after PEI in a rabbit VX2 liver tumor model. Magn Reson Imaging 2016;34:177–82.

[27] Jia WR, Tang L, Wang DB, et al. Three-dimensional contrast-enhanced ultrasound in response assessment for breast cancer: a comparison with dynamic contrast-enhanced magnetic resonance imaging and pathology. Sci Rep 2016;6:33832.

[28] Barnes SL, Whisenant JG, Loveless ME, et al. Practical dynamic contrast enhanced MRI in small animal models of cancer: data acquisition, data analysis, and interpretation. Pharmaceutics 2012;4:442–78.

[29] Baumgart DC, Bokemeyer B, Drabik A, et al. Vedolizumab induction therapy for inflammatory bowel disease in clinical practice—a nationwide consecutive German cohort study. Aliment Pharmacol Ther 2016;43:1090–102.

[30] Reigada LC, Hoogendoorn CJ, Walsh LC, et al. Anxiety symptoms and disease severity in children and adolescents with Crohn disease. J Pediatr Gastroenterol Nutr 2015;60:30–5.

[31] Eder P, Lykowska-Szuber L, Iwanik K, et al. The influence of anti-TNF therapy on CD31 and VEGF expression in colonic mucosa of Crohn's disease patients in relation to mucosal healing. Folia Histochem Cytobiol 2016;54:75–80.

[32] Jerkic M, Peter M, Ardelean D, et al. Dextran sulfate sodium leads to chronic colitis and pathological angiogenesis in Endoglin heterozygous mice. Inflamm Bowel Dis 2010;16:1859–70.

[33] Linares PM, Chaparro M, Gisbert JP. Angiopoietins in inflammation and their implication in the development of inflammatory bowel disease. A review. J Crohns Colitis 2014;8:183–90.

[34] Deban L, Correale C, Vetrano S, et al. Multiple pathogenic roles of microvasculature in inflammatory bowel disease: a Jack of all trades. Am J Pathol 2008;172:1457–66.

[35] Cui B, Feng Q, Wang H, et al. Fecal microbiota transplantation through mid-gut for refractory Crohn's disease: safety, feasibility, and efficacy trial results. J Gastroenterol Hepatol 2015;30:51–8.

[36] Vaughn BP, Vatanen T, Allegretti JR, et al. Increased intestinal microbial diversity following fecal microbiota transplant for active Crohn's disease. Inflamm Bowel Dis 2016;22:2182–90.

[37] Sinha R, Verma R, Verma S, et al. MR enterography of Crohn disease: part 2, imaging and pathologic findings. AJR Am J Roentgenol 2011;197:80–5.

[38] Nylund K, Jirik R, Mezl M, et al. Quantitative contrast-enhanced ultrasound comparison between inflammatory and fibrotic lesions in patients with Crohn's disease. Ultrasound Med Biol 2013;39: 1197–206.

[39] Park HS, Han JK, Lee JM, et al. Dynamic contrast-enhanced MRI using a macromolecular MR contrast agent (P792): evaluation of antivascular drug effect in a rabbit VX2 liver tumor model. Korean J Radiol 2015;16:1029–37.

[40] Tudorica A, Oh KY, Chui SY, et al. Early prediction and evaluation of breast cancer response to neoadjuvant chemotherapy using quantitative DCE-MRI. Transl Oncol 2016;9:8–17.